"Structure Breaking" Effect of Hydrated Cs^+

Christian F. Schwenk, Thomas S. Hofer, and Bernd M. Rode*

Institute of General, Inorganic and Theoretical Chemistry, University of Innsbruck, Innrain 52a, A-6020 Innsbruck, Austria

Received: October 21, 2003; In Final Form: December 11, 2003

Structural and dynamical properties of the hydrated Cs^+ ion have been investigated by performing ab initio quantum mechanical/molecular mechanical (QM/MM) molecular dynamics (MD) simulations at different quantum mechanical levels (HF, B3LYP and BP86). The first shell coordination number was found to be ∼8 in the HF and ∼9 in the B3LYP and BP86 case and several other structural parameters such as angular distribution functions, radial distribution functions, and tilt- and θ-angle distributions allowed to fully characterize the hydration structure of the Cs^+ ion. Velocity autocorrelation functions were used to calculate librational and vibrational motions, ion−ligand motions, as well as reorientation times. The strong "structure breaking" effect of Cs^+ can be interpreted on the basis of different dynamical parameters such as accelerated water reorientation, mean ligand residence time, and the number of ligand exchange processes.

1. Introduction

The structural lability of the Cs^+ ion in aqueous solution makes it very difficult to determine even rough data as average coordination numbers or the geometry of the hydrate complex formed. It is even more difficult for experimentalists to obtain reliable data for dynamical properties as ligand exchange rates, mean ligand residence times, or frequency shifts of this "structure breaking" alkaline metal ion by suitable experimental techniques. The problems are caused by the accessible time-scale of experimental methods and by the special features of the cation itself.[1]

X-ray diffraction studies of cesium salts at concentrations of 5.56 and 2.78 M yielded average coordination numbers of 3.04 and 5.75 showing a strong decrease of the coordination number with increasing concentration.[2] In previous X-ray diffraction experiments, the conclusion was drawn that, in dilute solutions, the coordination number of the cesium ion should be eight, whereas in concentrated solution, it should drop to about four.[3] The Cs−O distances measured experimentally vary between 3.1 and 3.3 Å. A molecular dynamics simulation performed on the cesium−water system at 25 °C using the TIP4P water model for water and the TIPS potential for the ion−water interactions yielded a coordination number of ∼10 and a Cs−O distance of 3.25 Å.[4] Using the SPC/E model for water and ion−water parameters fitted to the binding energies of small clusters of hydrated ions yielded a Cs^+−O distance of 3.05 Å and coordination numbers of 9.6[5] and 8.3[6] for the first and 21.3 for the second coordination shell.[5]

Several recent investigations of similar systems[7−9] have proven that QM/MM simulations improve the description of hydrated ions not only for the QM region itself but also the MM part, which is influenced by the structure of the first shell. Therefore, the above-mentioned parametrized classical models leading to quite different ligand distances and coordination numbers should be compared to results obtained by first principle methods.

Information on dynamic behavior of hydrated ions is still limited, especially for the very labile first and second row main group elements. Various techniques (NMR, quasielastic neutron scattering (QENS), and other relaxation techniques) have been employed in studies on dynamic properties of hydrated ions and rates of substitution of water molecules in the first and second hydration shell. The experimentally estimated rate constant for first shell water exchange of $\sim 10^{10}$ s^{-1} was obtained by NMR, which is usually restricted to a time range of $\geq 10^{-9}$ s (via bandwidths).

The ultrafast dynamics of hydrated Cs^+ is a very interesting challenge for both theory and experiment. Sufficiently accurate molecular dynamics (MD) simulations with a time step of 0.2 fs are a very promising tool to investigate water exchange reactions occurring in the subpicosecond time scale. Ab initio QM/MM MD simulations with sufficiently accurate quantum mechanical techniques (e.g., Hartree−Fock or hybrid density functionals) offer a good compromise between accuracy and simulation speed and, therefore, give a rather accurate access to fast-exchanging systems.

The way in which the structure of bulk waters is modified by the introduction of ions and the extent to which this determines the dynamical properties of the solution are important problems of liquid state chemistry. The surrounding of the ion can be divided into different regions: the innermost (primary) region where the water molecules are strongly oriented, the secondary region in which the molecules are only weakly oriented though the structure is broken down to a certain extent compared with bulk water, and finally the outermost region, far from the ion, exhibiting an identical structure as the bulk water.

The relative importance of these regions allows the classification of ions as "structure maker", which is the more common behavior, and as "structure breakers" observed especially for the alkaline metal ions K^+ and Cs^+. Water molecules in the primary region close to small and/or highly charged ions are strongly bound and such ions, therefore, are "structure makers" leading to well-defined ion−water complexes. In contrast, larger weakly interacting ions mainly disrupt the

* To whom correspondence should be addressed. E-mail: Bernd.M.rode@uibk.ac.at. Phone: +43-512-507-5160. Fax: +43−512-507-2714.

10.1021/jp037179v CCC: $27.50
Published on Web 02/10/2004

TABLE 1: Optimized Parameters for the Cs−O and Cs−H Two-Body Interaction (Energies in kcal mol^{-1})

	A	*B*	*C*	*D*
Cs−O	−5399.59	209691.46	−255683.30	12858.14
Cs−H	395.07	15506.44	−116883.02	523320.45

TABLE 2: Cs−O Distances in Å and Energies in kcal mol^{-1} for Cs−H_2O Clusters of Different Size Obtained from HF, MP2, B3LYP, and BP86 Calculations, BSSE Corrected Values in Parentheses

	r_{Cs-O}				dE_{ab}			
n	HF	MP2	B3LYP	BP86	HF	MP2	B3LYP	BP86
1	3.13	3.12	3.08	3.11	−14.0 (13.5)	−14.4 (13.5)	−14.5 (13.4)	−14.0
2	3.16	3.15	3.12	3.14	−26.9	−27.8	−28.0	−27.2
3	3.17	3.17	3.13	3.15	−38.5	−39.9	−40.5	−39.4
4	3.21	3.20	3.16	3.18	−48.6	−50.6	−51.3	−50.1
6	3.29	3.26	3.23	3.25	−63.6	−66.8	−67.7	−66.6
8	3.37	3.34	3.32	3.35	−71.4	−76.3	−76.3	−75.2

hydrogen bonding network characteristic for bulk water but have only a rather weak influence on the orientation of the water molecules in their closest neighborhood. The net effect of these ions is "structure breaking", therefore, which can be recognized from ligand orientation times shorter than for the pure solvent.[1]

The main motivation of this work was to find answers to the structural ambiguities and to obtain accurate data for dynamic properties of the highly labile Cs^+ hydrate.

2. Methods

The pair potential for Cs^+ water was newly constructed using DZP basis sets for H_2O[10] and the LANL2DZ effective core potential (ECP)[11] basis set for Cs^+. 4300 Hartree−Fock interaction energy points obtained by the TURBOMOLE 5.5 program[12−15] were fitted to the analytical form

$$E_{2bd} = \frac{q_O q_{Cs}^I}{r} + \frac{A_O}{r^5} + \frac{B_O}{r^8} + \frac{C_O}{r^9} + \frac{D_O}{r^{12}} + \sum_{i=1}^{2} \frac{q_H q_{Cs}^I}{r_i} + \frac{A_H}{r_i^5} + \frac{B_H}{r_i^7} + \frac{C_H}{r_i^9} + \frac{D_H}{r_i^{12}} \quad (1)$$

by a least-squares error minimization using the Levenberg−Marquardt algorithm. *A, B, C* and *D* are the fitting parameters (Table 1),

The values of −0.65966 and 0.32983 were adopted for q_O and q_H according to the flexible BJH−CF2 water model.[16,17] The experimental gas-phase geometry of water was fixed (O−H distance of 0.9601 Å and H−O−H angle of 104.47°). The global energy minimum was found to be −13.9 kcal mol^{-1}, and the average absolute residual of the fitted function was 0.22.

To detect possible error sources in pair potential and subsequent QM/MM calculations, calculations on $[Cs(H_2O)_n]^+$ clusters were performed, employing different levels of theory and estimating upper limits of the basis set superposition error (BSSE). Table 2 shows Cs−O distances and ab initio energies calculated for different cluster sizes $[Cs(H_2O)_n]^+$ ($n = 1-8$) at Hartree−Fock, MP2, and B3LYP levels. The results allow the effect of electron correlation to be demonstrated. The MP2 distances are slightly shorter than those from HF and larger than the B3LYP values due to the missing electron correlation in the HF case and its overestimation in the hybrid density functional method. A similar effect is observed for the ab initio energies, but here MP2 values are closer to the B3LYP data. Overall, however, it can be stated that the effects of electron correlation and BSSE should have only a minor influence on the QM/MM simulation quality.

The QM/MM technique[18,19,20] used in this work divides the system into a part (QM) treated by means of the respective quantum mechanical technique, whereas the rest of the system is described by means of classical molecular mechanics (MM). A smoothing function (ST2 switch) ensures a smooth and continuous transition from QM to MM forces. The system is described by the following formula:

$$F_{tot} = F_{MM}^{sys} + (F_{QM}^{QM} - F_{QM}^{MM})S(r) \quad (2)$$

where F_{tot} is the total force of the system, F_{MM}^{sys} is the MM force of the total system, F_{QM}^{QM} is the QM force in the QM region, and F_{QM}^{MM} is the MM force in the QM region. F_{QM}^{MM} accounts for the coupling between the QM and MM region. Our QM/MM program allows water molecules to leave and enter the QM region as needed.

Three different QM methods were employed in this work to investigate the influence of density functionals on structural and dynamical properties and the description of the "structure breaking" effect of hydrated Cs^+. Besides a Hartree−Fock simulation, the most common hybrid density functional technique B3LYP[21] and the pure density functional method BP86 were used.[22] The comparison of these conventional QM techniques in the QM/MM simulations should provide further data for the reliability of the respective technique to describe weakly hydrated ions.

All simulations were carried out with a simulation protocol similar to our previous work.[7,23,24] The simulations were carried out in a canonical *NVT* ensemble consisting of one Cs^+ and 499 water molecules in a cubic box of 24.6 Å. The simulation temperature of 298 K was kept constant using the Berendsen algorithm,[25] and the density of the system was assumed to be 0.997 g cm^{-3}, which is the density of pure water at the simulation temperature. The reaction field method[26] was employed to correct the cutoff of long-range electrostatic interactions. The Newtonian equations of motion were treated by a general predictor corrector algorithm and a time step of 0.2 fs was chosen, since the BJH−CF2 water model[16,17] allows explicit hydrogen movements.

A classical pair potential molecular dynamics simulation was performed first for 50 ps, starting from a random configuration. The combined QM/MM molecular dynamics simulations, in which the ion and its full first hydration shell were included into the QM region (QM radii of 5.0 Å for HF and 4.5 Å for B3LYP and BP86), started from the equilibrium configuration resulting from the pair potential simulation. After 2 ps of reequilibration, another 15 ps of sampling were performed in all three cases.

Besides structural properties as radial distribution functions, coordination numbers, and various angle distributions, dynamical properties such as water exchange rate constants, mean residence times of ligand molecules, vibrational and rotational motions, as well as ion-oxygen frequencies are of great interest, especially with regard to the extremely flexible "structure breaking" hydrate of the Cs^+ ion. Velocity autocorrelation functions give direct insight into the dynamics in a fluid system as the time integrals are related to macroscopic transport coefficients, and their Fourier transformations are directly related to vibrational spectra. The frequencies of vibrational and librational motions were obtained by normal-coordinate analysis.[27] Six scalar quantities Q_1, Q_2, Q_3, R_x, R_y, and R_z were defined to describe

the symmetric stretching vibration, bending vibration, asymmetric stretching vibration, and the rotations around the three principal axes of water molecules. The standard scaling factors of 0.89 and 0.96[28,29] were applied to scale the computed HF and DFT frequencies, respectively, to make them directly comparable with experimental data.

QM/MM MD simulations also allow us to investigate reorientational time correlation functions (RCTFs) defined as

$$C_{li}(t) = \langle P_l(\vec{u}_i(0)\vec{u}_i(t))\rangle \quad (3)$$

where P_l is the Legendre polynomial of lth order and $\vec{u}_i$ is a unit vector along three principal axes i defined in a fixed coordinate frame as the rotations above. The RCTFs were fitted to the simple form

$$C_l(t) = a\exp(-t/\tau_1) \quad (4)$$

where a and τ_1 are the fitting parameters, and τ_1 is the corresponding relaxation time.

Many first shell exchange processes have been observed within the simulation time of 15 ps. In a previous investigation,[30] we have compared two different evaluation methods for mean ligand residence times, namely the "direct" method, accounting for all actually incoming and outgoing ligands, and the procedure suggested by Impey et al.,[31] based on a "survival function". This work has shown that the usage of a full accountancy of all ligand movements ("direct" method) seems to be advantageous and that the most appropriate time span to record a ligand displacement from its original coordination sphere as an exchange process is 0.5 ps (this time also corresponds to the average lifetime of a hydrogen bond in the solvent[32]).

Simulation data can provide further information concerning the lability of the hydration shell, measurable by the number and "sustainability" of ligand exchange processes. It is possible to measure the number of exchange events leading to a longer-lasting change in the hydration structure by comparing the number of transitions through a shell boundary (N_{ex}^0), to the number of changes persisting after 0.5 ps ($N_{ex}^{0.5}$), defining a sustainability coefficient

$$S_{ex} = N_{ex}^{0.5}/N_{ex}^0$$

Its inverse ($1/S_{ex}$) accounts how many border-crossing attempts are needed to produce one longer-lasting change in the hydration structure of an individual ion.[30]

3. Results and Discussion

3.1. Structure. The Cs−O RDFs (Figure 1) already give clear indications toward the "structure breaking" behavior of the ion: the broad asymmetric first-shell peak, a very flat but still recognizable second shell, and numerous small inter-shell peaks are typical for a very flexible and quite irregular structure of the hydrate with rapidly changing ligand coordinations. These properties have been observed in a similar but much less pronounced way for K^+.[9] Not much difference is observed between the three QM methods. The intershell region is less populated with HF, moving one ligand from the first shell area to the second shell in comparison to the DFT methods.

The first shell peak maxima are located at 3.25 (HF), 3.20 (B3LYP), and 3.30 Å (BP86) in very good agreement with several experimental results (3.22−3.30 Å[3]). In contrast to our previous work investigating Ca^{2+},[23] no contraction of the hydrate complex was observed in the DFT cases compared to HF, most probably due to the extraordinary high flexibility of the water molecules surrounding the cesium ion, which allows even first-shell ligands to orient themselves in favor of the stronger H-bonding between ligands in the DFT formalism.

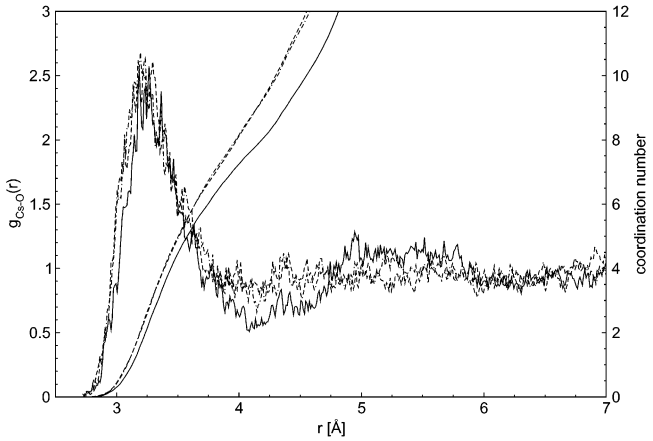

Figure 1. Cs-O radial distribution functions and their running integration numbers: HF/MM (solid line), B3LYP/MM (dashdotted line), and BP86/MM (dashed line).

TABLE 3: Hydration Structure Parameters of Cs^+ in Water Determined by QM/MM Molecular Dynamics Simulations

	HF/MM	B3LYP/MM	BP86/MM
$r_{1,\,max}$ [Å][a]	3.25	3.20	3.30
$r_{1,\,min}$ [Å]	∼4.1	∼4.2	∼4.2
$r_{2,\,max}$ [Å][b]	∼5.2	∼5.2	∼4.4
$r_{2,\,min}$ [Å]	∼6.0	∼6.0	∼6.0
CN^{first} [c]	7.8	8.9	9.1
CN^{second}	∼20	∼18	∼24
mean O−M^{2+}−O angle [°]	56/94	46/87	44/73
mean θ angle [°][d]	132	128	125
mean tilt angle [°][e]	−55/35	−40/55	−55/55
mean α(O−H−O) [°]	105.0	104.0	103.0
mean d(O−H) [Å]	0.952	0.977	0.987

[a] First peak maximum of Cs^+−O−RDF; exp. values: 3.22−3.30 Å.[3] [b] Second peak maximum of Cu^+−O−RDF. [c] First shell coordination number; exp. values: 6−7.9.[3] [d] Angle between ion−O and dipole vector. [e] Angle between ion−O vector and water plane.

Comparing these results with those of the classical models, it seems that the TIPS/TIP4P model[4] overestimates the coordination number, whereas the SPC/E[5] model strongly underestimates the ion-ligand distance.

The minima between first and second hydration shell are not well defined (Table 3), especially in the DFT case, but the differentiated RDF makes it possible to locate the borderline of the first hydration shell within ±0.1 Å and thus to determine coordination numbers with an accuracy of ±0.4.

The second hydration shell is very broad without showing clear maxima in all cases, and it is very difficult, therefore, to determine the peak maxima (see Table 3). The HF method defines the second coordination shell best with a clearly defined minimum between first and second shell, in contrast to the DFT results yielding a much weaker structurization outside the first shell (Figure 1), indicating a possible inadequacy of pure DFT methods.

The average second shell distances of HF and B3LYP are very similar (∼5.2 Å), whereas in the pure DFT technique BP86 a clear shift toward the cation was observed (∼4.4 Å).

The minima between second shell and bulk are much less defined making it difficult to distinguish the second shell. However, all RDFs in Figure 1 indicate a transition from a weakly structured region to a rather uniform bulk structure around 6 Å. Therefore, second shell coordination numbers are

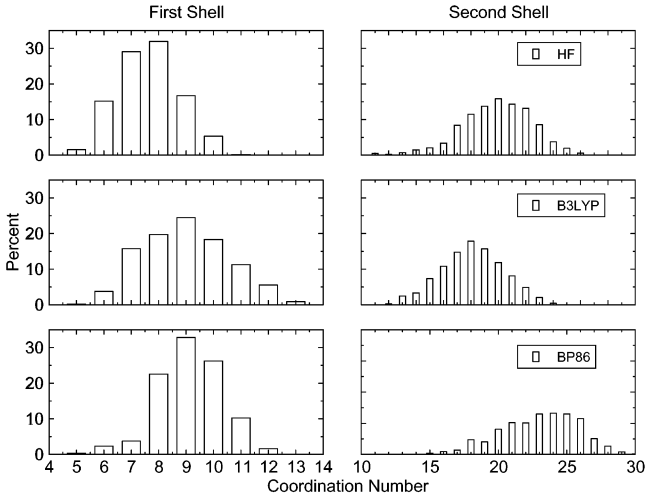

Figure 2. Coordination number distributions of the first and second hydration shell: HF/MM, B3LYP/MM, and BP86/MM simulation.

rather approximate values. Experimental data for Cs^{+} [3] and similar ions as K^{+} [33] and Rb^{+} [34] do not prove the presence of a clearly defined second hydration shell, which is basically in agreement with our simulation data. Simulations have the advantage, however, to allow the detection of weak structurisations, which are hardly visible under the energy impact of diffraction methods and thus allow us to describe effects related to such structural entities.

The coordination number distribution for first and second hydration shell is shown in Figure 2 for HF, B3LYP, and BP86.

The first shell coordination number of the HF/MM simulation is significantly smaller compared to the DFT/MM simulations, in contrast to other DFT simulations, such as Car-Parinello calculations, which generally tend to underestimate coordination numbers, yielding for example a coordination number of 5 for Cu^{2+}.[35] In the case of cesium, the most probable reason for the high coordination numbers obtained with hybrid as well as pure density functional simulations is the very low Cs^{+}−water binding energy which enhances the relative importance of the hydrogen bonding between the ligands.

The very broad coordination number distributions (see Figure 2) gives another indication toward the extremely fast dynamics in the first hydration shell due to the "structure breaking" effect of Cs^{+}. The range of the first-shell coordination number is 5−10 in the HF/MM case and 6−12 in the DFT/MM cases, which means coexistence of a wide variety of different species. Comparing the hybrid B3LYP first shell coordination number distribution with BP86, the distribution is obviously broader in the B3LYP case, indicating higher flexibility in the first hydration shell. The second shell maximum with BP86 at a much shorter distance, but associated with a much higher coordination number, is a further indicator for the limited suitability of pure DFT methods for the description of hydrated ions. The average first shell coordination numbers are 7.8 (HF), 8.9 (B3LYP), and 9.1 (BP86) showing the 8-fold coordinated complex to be dominant in the HF/MM case and the 9-fold coordinated species using density functionals. The second shell coordination number is very difficult to estimate due to the very diffuse and broad peak. However, an approximate coordination number of ∼20 can be assumed for the cesium ion, showing a slight dominance of the higher coordinated species in the HF case (20) compared to the DFT B3LYP results (18), 24 resulting from BP86 seems clearly overestimated.

The angular distribution functions (O−Cs−O angle) are shown in Figure 3 for three different QM/MM MD simulations.

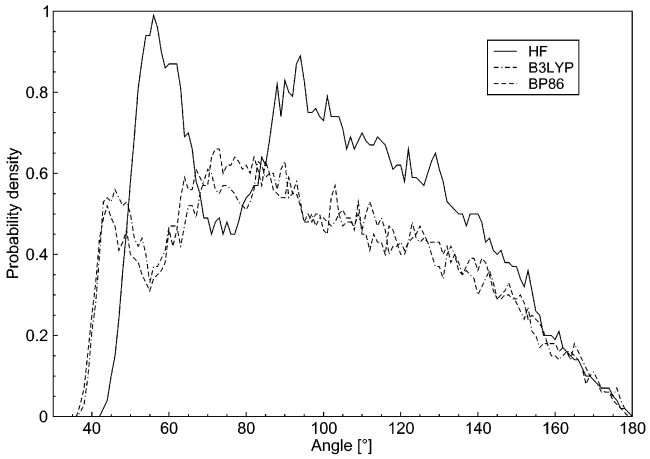

Figure 3. Angular distribution functions (O−Cs−O) of the first shell obtained from three different QM/MM MD simulations at HF, B3LYP, and BP86 level.

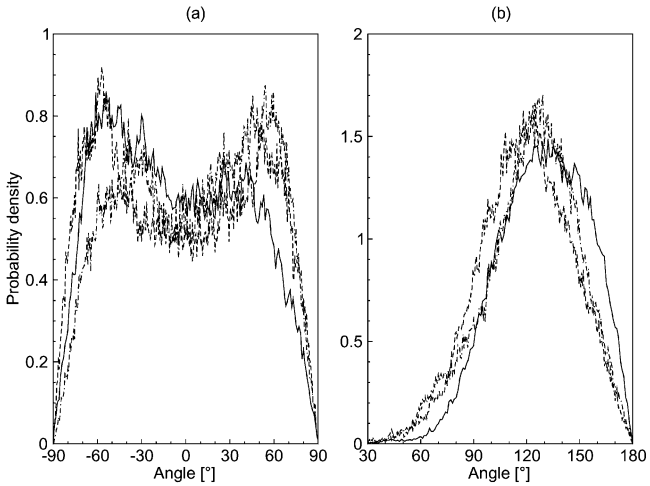

Figure 4. Angular Cs−H_2O configuration: (a) Tilt angle and (b) θ angle distributions (for definitions see main text) obtained from three different QM/MM MD simulations at HF (solid line), B3LYP (dash-dotted line), and BP86 level (dashed line).

Two peaks were observed in all three cases, but they are shifted and more pronounced in the HF case due to the lower coordination. By no means, any regular symmetric structure can be identified.

It is also interesting to investigate the relative positions of the water molecules surrounding the Cs^{+} ion, to compare the three QM/MM simulation techniques in more detail and to investigate the influence of the "structure breaking" effect. Therefore, two different angles were defined: the θ angle is defined as the angle between the Cs−O connection vector and the vector resulting from the sum of the O−H vectors, and the tilt angle is the angle between the Cs−O vector and the plane defined by the O−H vectors. Tilt and θ angle distributions are depicted in Figure 4, parts a and b.

The mean tilt angles are very similar for the three QM/MM simulations showing two maxima at −55/35° (HF), −40/55° (B3LYP), and −55/55° (BP86) as listed in Table 3. The same similarity was observed for the θ angles peaking at ∼120°. Such strongly tilted arrangements with rather small θ angles were not found for other more strongly interacting transition metal ions[23,7] and can thus be considered another characteristic feature of a "structure breaking" ion.

3.2. Dynamics. *3.2.1. Velocity Autocorrelation Functions.* The frequencies for the librational motions R_x, R_y, and R_z,

TABLE 4: Vibrations, Librations, and Ion−O Stretching Modes of First Shell Waters Obtained from QM/MM MD Simulations of Cs^+ in Water (Frequencies in cm^{-1}; Numbers in Parentheses Correspond to Bulk Phase (MM) Values)

method	R_z[a]	R_x	R_y	Q_2[b]	Q_1	Q_3	Q_{iO}[c]
HF/MM	413	377	519	1655	3572	3661	100
				(1698)	(3452)	(3556)	
B3LYP/MM	461	437	576	1673	3499	3604	100
				(1698)	(3452)	(3567)	
BP86/MM	444	434	572	1637	3369	3475	105
				(1699)	(3451)	(3560)	
EXP.[d]				1648	3714	3769	
H_2O(BJH)[e]	415	420	540	1698	3455	3552	
H_2O(exp.)[f]				1645	3345	3445	
H_2O(gas)[g]				1610	3650	3768	

[a] R_x, R_y, and R_z denote the librational frequencies of rotation around the three principal axes of the water molecule. [b] Q_1, Q_2, and Q_3 denote the frequencies of the symmetric stretching, bending, and asymmetric stretching vibrations of the water molecule. [c] Stretching mode of the ion-oxygen motion. [d] Experimental data from ref 36. [e] Pure liquid simulation with the BJH water model.[17] [f] Experimental values for liquid water.[37] [g] Scaled HF values.

TABLE 5: Reorientational Times of First Shell and Mean Residence Times of Second Shell Waters Obtained from QM/MM MD Simulations of Cs^+ in Aqueous Solution (Times in ps)

	HF/MM	B3LYP/MM	BP86/MM	H_2O(BJH)[a]	H_2O(exp.)
τ_{1x}[b]	1.1	2.3	1.9	4.8	7.5[c]
τ_{1y}	0.9	1.9	1.6	5.7	
τ_{1z}	1.4	2.9	2.4	6.6	
τ_{2x}	0.5	1.2	1.0	2.6	2.5[c]
τ_{2y}	0.4	0.9	0.9	2.9	
τ_{2z}	0.4	1.0	1.0	3.3	

[a] Pure liquid simulation with the BJH water model.[17] [b] Reorientational times about the three principal axes *x*, *y*, and *z* of first and second order. [c] Experimental reorientational correlation time of water.[40]

obtained from the power spectra of velocity autocorrelation functions (VACFs) using the normal mode approximation[38] are listed in Table 4. Previous investigations of Ni^{2+},[27] Mn^{2+}, and V^{2+} [39] yielded the order $R_z < R_x < R_y$. However, the inhomogeneous R_y and R_z plots of the QM/MM MD simulation of Cs^+ in water caused by different configurations occurring throughout the simulations did not allow us to give a unique order for the librational motions. The R_x values show the lowest inhomogeneity in all cases and the R_y values are clearly larger than the R_x and R_z frequencies. The results obtained for both DFT techniques B3LYP and BP86 are very similar showing significantly higher wavenumbers for the rotations around the three principal axis than the HF method, which corresponds to a higher rigidity of the hydrate complex. Overall, however, the "structure breaking" effect of Cs^+ leads to broad peaks with several shoulders due to the different species coexisting in the hydration shell and making it rather difficult to give accurate values for the rotational wavenumbers.

Rotational relaxation times (see Table 5) allow us to study the rotational properties of water molecules under the influence of a cation.

The correlation functions for $l = 1$ are related to IR lines and for $l = 2$ to Raman line shapes and NMR relaxation.[40,22] The highest relaxation times are found for rotations around the *z* axis, and consequently, this is the most stable axis so that a rotation around this dipole axis is the most probable movement besides translation in each case. The "structure breaking" effect of the Cs^+ leads to reorientational times considerably smaller than those for pure water, for both τ_1 and τ_2.

The first shell vibrational motions of water molecules Q_1, Q_2, and Q_3 are listed in Table 4. The frequencies in the bulk are consistent with previously obtained data from MD simulations[38,41] and experimental values.[37] All bending frequencies are slightly red-shifted compared to the bulk, showing the largest shift in the BP86/MM case. The stretching frequncies of the HF/MM simulation are blue-shifted and the nearly unchanged B3LYP/MM frequencies are also slightly blue-shifted in contrast to the BP86/MM simulation showing clearly red-shifted stretching frequncies. Overall, the similar results for HF and B3LYP show a possible error source of pure DFT techniques for describing hydrated metal ions.

TABLE 6: Mean Ligand Residence Times, Number of Accounted Ligand Exchange Events, and Sustainability of Migration Processes to and from the First Hydration Shell of Cs^+ in ps

	HF/MM	B3LYP/MM	BP86/MM	HF/MM (pure H_2O)
$N_{ex}^{0.5}$/10 ps[a]	51	40	47	24
τ_D[b]	1.5	2.2	1.9	1.7
S_{ex}[c]	0.3	0.2	0.2	0.1
$1/S_{ex}$[d]	2.9	4.7	5.1	11.2

[a] Number of accounted exchange events. [b] Mean ligand residence time determined by the direct method[30] in ps. [c] Sustainability of migration processes. [d] Number of processes needed for one successful ligand exchange.

The QM/MM technique also allows us to calculate the ion−oxygen frequencies and the corresponding bond strengths. The Cs−O frequency obtained with our QM/MM simulations is $\sim$100 cm^{-1} independent of the simulation technique. The corresponding force constant is $\sim$8.5 Nm^{-1} proving a very weak interaction of the ion with its closest environment, which together with the size of the hydrate, contributes to the "structure breaking" effect.

3.2.2. Interpretation of the "Structure Breaking" Effect of Cs^+. The "structure breaking" effect means on a microscopic scale that the thermal motions of the water molecules near the ion occur faster than in pure water. The reorientation times of Table 5 have illustrated this behavior impressively and shown that QM/MM simulations are capable of reproducing such details. In addition to that, QM/MM MD simulations are a very suitable tool to characterize ultrafast ligand dynamics as in the case of Cs^+ which experiences an extraordinary high number of water exchange processes compared to other cations. Table 6 lists some of the most important dynamical parameters as the number of ligand exchange processes, the mean ligand residence times and the sustainability of migration processes between first and second hydration shell.

The number of accounted exchange events normalized to 10 ps simulation time, $N_{ex}^{0.5}$, is approximately twice the number observed for pure water. This is a clear indication for a strongly enhanced mobility of first shell water molecules neighboring the cation and thus confirms further the nature of the "structure breaking" effect of Cs^+. The first-shell mean ligand residence times calculated from the "direct" method are very similar for the three QM/MM simulations of Cs^+ in water and considerably smaller than MRTs calculated from classical MD simulations of hydrated Cs^+ yielding a value of $\sim$10 ps[6] using the Impey formalism.[31]

The experimentally estimated rate constant for first shell water exchange based on NMR[42,43] data is nearly 2 orders of magnitude smaller with $\sim 10^{10}$ s^{-1} than the result obtained from our QM/MM simulations, $\sim 10^{12}$ s^{-1} (for HF, hybrid B3LYP and pure density functional technique BP86).

The very fast ligand exchange behavior of Cs^+ in aqueous solution is beyond the time scale of NMR measurements

(estimations by line-widths are limited to $\geq 10^{-9}$ s), and therefore, all experimental exchange rates below this value have been classified as estimations by the authors.[42] The time step of 0.2 fs used in our simulations allows us to predict dynamical processes in the femtosecond range. Previous ab initio QM/MM MD simulations of several similar systems, including pure water, have yielded adequate MRTs, proving the suitability of this methodology to describe ultrafast dynamics.[30]

The sustainability of migration processes is also accessible from our QM/MM MD simulations, and its reciprocal value gives the number of processes needed for one successful ligand exchange. The smallest $1/S_{ex}$ value was obtained for the HF/MM, and slightly higher values for both DFT/MM and all of them are considerably lower than the corresponding pure water. This means that ligand exchange processes are facilitated in the presence of Cs^+ and that a smaller number of attempts is sufficient to accomplish an exchange. This compensates the water binding ability of the ion and leads, therefore, to a mean residence time equal or even slightly shorter than in the solvent itself.

4. Conclusion

From a methodical viewpoint the simulations performed for Cs^+ in water by 3 different quantum mechanical methods confirm that pure density functional methods are not adequate for the description of hydrated ions, even weakly interacting ions, but that the hybrid density functional method B3LYP seems to be a suitable alternative to ab initio HF treatment of the QM region (albeit without any time-saving effect).

The simulations have produced a very detailed picture of the "structure breaking effect" of a large, weakly interacting cation, which comprises a number of interrelated effects: a quite irregular first hydration shell composed of several, rapidly changing species, in which water reorientation times are considerably faster than in the solvent itself, a very fast ligand exchange between first and second hydration sphere, and a not well-ordered but highly space-consuming second shell, thus disrupting the solvent's H bonded structure are the main features. These features can satisfactorily explain the experimental observations related to "structure breaking" of such ions in aqueous solutions and supply further details for the reasons of this behavior.

Acknowledgment. Financial support for this work from the Austrian Science Foundation (FWF) is gratefully acknowledged (Project P16221-NO8).

References and Notes

(1) Hertz, H. G. *Water: A Comprehensive Treatise*; Plenum Press: New York, 1973; Vol. 3.
(2) Tamura, Y.; Yamguchi, T.; Okada, I.; Ohtaki, H. *Z. Naturforsch. A* **1987**, *42* (4), 367.
(3) Smirnov, P. R.; Trostin, V. N. *Rus. J. Phys. Chem.* **1995**, *69* (7), 1218−1223.
(4) Lee, S. H.; Rasaiah, J. C. *J. Chem. Phys.* **1994**, *101* (8), 6964−6974.
(5) Lee, S. H.; Rasaiah, J. C. *J. Phys. Chem.* **1996**, *100* (4), 1420−1425.
(6) Koneshan, S.; Rasaiah, J. C.; Lynden-Bell, R. M.; Lee, S. H. *J. Phys. Chem. B* **1998**, *102* (21), 4193−4204.
(7) Loeffler, H. H.; Rode, B. M. *J. Chem. Phys.* **2002**, *117* (1), 110−117.
(8) Tongraar, A.; Liedl, K. R.; Rode, B. M. *Chem. Phys. Lett.* **1998**, *286*, 56−64.
(9) Tongraar, A.; Liedl, K. R.; Rode, B. M. *J. Phys. Chem. A* **1998**, *102* (50), 10340−10347.
(10) Dunning, T. H., Jr. *J. Chem. Phys.* **1970**, *53* (7), 2823−2833.
(11) Wadt, W. R.; Hay, P. J. *J. Chem. Phys.* **1985**, *82*, 284−298.
(12) Ahlrichs, R.; Bär, M.; Häser, M.; Horn, H.; Kölmel, C. *Chem. Phys. Lett.* **1989**, *162* (3), 165−169.
(13) Brode, S.; Horn, H.; Ehrig, M.; Moldrup, D.; Rice, J. E.; Ahlrichs, R. *J. Comput. Chem.* **1993**, *14* (10), 1142−1148.
(14) Ahlrichs, R.; von Arnim, M. In *Methods and Techniques in Computational Chemistry: METECC-95*; Clementi, E., Corongiu, G., Eds.; STEF: Cagliari, 1995; Chapter 13, pp 509−554.
(15) von Arnim, M.; Ahlrichs, R. *J. Comput. Chem.* **1998**, *19* (15), 1746−1757.
(16) Stillinger, F. H.; Rahman, A. *J. Chem. Phys.* **1978**, *68* (2), 666−670.
(17) Bopp, P.; Janscó, G.; Heinzinger, K. *Chem. Phys. Lett.* **1983**, *98* (2), 129−133.
(18) Gao, J. In *Reviews in Computational Chemistry*; Lipkowitz, K. B., Boyd, D. B., Eds.; VCH Publishers: New York, 1996; Vol. 7, Chapter 3, pp 119−185.
(19) Gao, J. *Acc. Chem. Res.* **1996**, *29* (6), 298−305.
(20) Bakowies, D.; Thiel, W. *J. Phys. Chem.* **1996**, *100* (25), 10580−10594.
(21) Becke, A. D. *Phys. Rev. A* **1988**, *38* (6), 3098−3100.
(22) Allen, M. P.; Tildesley, D. J. *Computer Simulation of Liquids*; Oxford Science Publications: New York, 1990.
(23) Schwenk, C. F.; Loeffler, H. H.; Rode, B. M. *J. Chem. Phys.* **2001**, *115* (23), 10808−10813.
(24) Inada, Y.; Mohammed, A. M.; Loeffler, H. H.; Rode, B. M. *J. Phys. Chem. A* **2002**, *106* (29), 6783−6791.
(25) Berendsen, H. J. C.; Postma, J. P. M.; van Gunsteren, W. F.; DiNola, A.; Haak, J. R. *J. Phys. Chem.* **1984**, *81*, 3684−3690.
(26) Adams, D. J.; Adams, E. M.; Hills, G. J. *Mol. Phys.* **1979**, *38* (2), 387−400.
(27) Inada, Y.; Loeffler, H. H.; Rode, B. M. *Chem. Phys. Lett.* **2002**, *358*, 449−458.
(28) Scott, A. P.; Radom, L. *J. Phys. Chem.* **1996**, *100*, 16502−16513.
(29) DeFrees, D. J.; McLean, A. D. *J. Chem. Phys.* **1985**, *82* (1), 333−341.
(30) Hofer, T. S.; Tran, H. T.; Schwenk, C. F.; Rode, B. M. *J. Comput. Chem.* **2004**, *25*, 211−217.
(31) Impey, R. W.; Madden, P. A.; McDonald, I. R. *J. Phys. Chem.* **1983**, *87* (25), 5071−5083.
(32) Lock, A. J.; Woutersen, S.; Bakker, H. J. *Femtochemistry and Femtobiology*; World Scientific: Singapore, 2001.
(33) Neilson, G. W.; Skipper, N. *Chem. Phys. Lett.* **1985**, *114*, 35−38.
(34) Ramos, S.; Barnes, A. C.; Neilson, G. W.; Capitan, M. J. *Chem. Phys.* **2000**, *258*, 171−180.
(35) Pasquarello, A.; Petri, I.; Salmon, P. S.; Parisel, O.; Car, R.; Tóth, É.; Powell, D. H.; Fischer, H. E.; Helm, L.; Merbach, A. *Science* **2001**, *291*, 856−859.
(36) Ushanova, N. I.; Aleksandrovskaya, A. M.; Kotomina, R. A. *Rus. J. Phys. Chem.* **1982**, *56* (2), 278−279.
(37) Murphy, W. F.; Bernstein, H. J. *J. Phys. Chem.* **1972**, *76* (8), 1147−1152.
(38) Bopp, P. *Chem. Phys.* **1986**, *106* (205−212).
(39) Schwenk, C. F.; Loeffler, H. H.; Rode, B. M. *J. Am. Chem. Soc.* **2003**, *125*, 1618−1624.
(40) Ohtaki, H.; Radnai, T. *Chem. Rev.* **1993**, *93* (3), 1157−1204.
(41) Spohr, E.; Pálinkás, G.; Heinzinger, K.; Bopp, P.; Probst, M. M. *J. Phys. Chem.* **1988**, *92* (23), 6754−6761.
(42) Helm, L.; Merbach, A. E. *Coord. Chem. Rev.* **1999**, *187*, 151−181.
(43) Lincoln, S. F.; Merbach, A. In *Advances in Inorganic Chemistry*; Academic Press: New York, 1995; Vol. 42, pp 1−88.